ACS APPLIED MATERIALS & INTERFACES

Research Article

www.acsami.org

# Porous Surface Structure Fabricated by Breath Figures that Suppresses *Pseudomonas aeruginosa* Biofilm Formation

Kengo Manabe, Shingo Nishizawa, and Seimei Shiratori*

Graduate School of Science and Technology, School of Integrated Design Engineering, Keio University, 3-14-1 Hiyoshi, Kohoku-ku, Yokohama, Kanagawa 223-8522, Japan

Supporting Information

**ABSTRACT:** As colonizers of medical-device surfaces, *Pseudomonas aeruginosa* strains present a serious source of infection and are of major concern. In this study, we fabricated films with porous surfaces by breath figures that disturb mergence by bacterial attachment, thereby impeding biofilm development. Previous studies have shown that microtopography prevents the development of *P. aeruginosa* biofilms. Accordingly we indented surfaces with patterns of micrometer-sized pores using breath figures at ordinary temperatures and pressures. The antimicrobial effect of surface figures was experimentally investigated by controlling the surface structure. The results suggested that pores of 5−11 μm in diameter effectively inhibit bacterial activity. It appears that biofilm development is precluded by the decreased contact area between the films and bacteria.

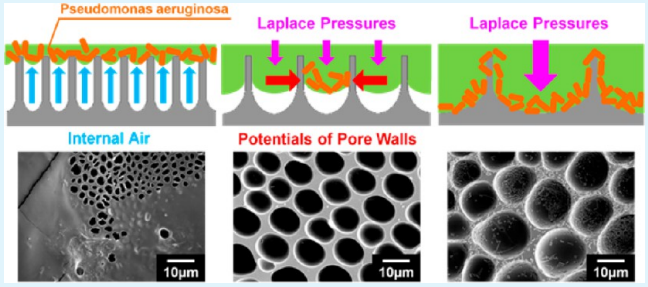


**KEYWORDS:** *breath figures, self-organization, antibacterial, microtopography, surface structure, biofilms*

## INTRODUCTION

With increasing emphasis on human hygiene, the removal of microorganisms that threaten human health has gained considerable attention in recent years.[1−5] These concerns are particularly urgent in the medical fields because widely used medical equipment, such as T-shape stopcocks, is readily colonized by microorganisms.[6,7] Inhibition of bacterial settlement or growth is necessary to prevent the spread of deadly diseases by contact and aerial infection.[8,9] Such prohibitive measures must target biofilms, which promote microbial aggregation and growth.[10,11] One promising prophylaxis approach is antibacterial coating.[12,13]

Antibacterial films may be fabricated in two ways. Surfaces may be coated with antimicrobial chemicals[14,15] or imprinted with an indented pattern that discourages bacterial adhesion.[16,17] Although the former approach generally exerts a significant antibacterial effect, it not only requires costly drugs or materials (such as Ag particles) but also encourages the emergence of drug-resistant mutations, with potentially devastating effect on human health.[18,19] Conversely, because the latter approach erects a physical rather than a chemical barrier, it should not induce genetic changes that lead to resistant strains.[20] The geometric approach is especially promising for species such as *Pseudomonas aeruginosa*, which exhibits excellent drug tolerance.[21−23]

The disadvantage of the geometric approach is the high energy and cost of manipulating the etching equipment in a vacuum. At present, vacuum application is required to realize the high precision necessary for microstructural control of the surface. In addition, previously fabricated geometric antimicrobial films encouraged bacterial cohesion and growth in the micropillars formed on the bottom surfaces of the substrate. As a matter of course, it was confirmed that the smooth surface cannot inhibit bacterial adhesion.[24,25] To our knowledge, few studies have used the geometric approach to inhibit *P. aeruginosa* proliferation by limiting the organic substance traces through which the cells coordinate their movements.

Therefore, we aimed to fabricate antibacterial thin films at reduced energy and cost by introducing separated pores that preclude bacterial cohesion. Such films can readily accommodate a variety of features and are flexible in their use. The films were fabricated by breath figures, a method of generating porous structures at room temperature and normal pressure.[26−29]

Micrometer-sized 3D textured structures can be fabricated from nanometer-sized units by self-assembly and self-organization of macromolecules.[30−32] Representative examples are the Langmuir−Blodgett (LB) method,[33−35] the layer-by-layer (LbL) method,[36−38] microphase-separated block copolymer structures,[39−41] and mesoporous materials.[42−44] These self-assembling technologies use chemical processes to create a novel functional interface. The breath figure method casts polymer solution onto the substrate in a high-humidity environment, coating it with a highly ordered porous polymer film. The deposited film is characterized by regular arrays and uniform pore size, controlled from the nanometer to the

Received: August 26, 2013
Accepted: October 30, 2013
Published: October 30, 2013

  

micrometer scale by tuning the humidity, polymer concentration, polymer type, and molecular weight.[45−47]

Among the diverse potential applications of films fabricated by breath figures are cell culture substratum,[48] optical film,[49] and substance separation filter.[50]

Here, we report the first use of a porous thin film fabricated by breath figures as an antimicrobial agent. The target organism was *P. aeruginosa*, a notorious source of hospital infection.[51]

The experimental results of this study demonstrate the efficacy of antibacterial films with a micropatterned indented surface generated by breath figures. Furthermore, we establish the pore diameters that yield the strongest antibacterial effect and investigate their antimicrobial actions.

## EXPERIMENTAL SECTION

**Materials.** The materials used in this experiment were selected from the viewpoint of compatibility between the polymer and organic solvent.[52] Polystyrene (PS, $M_w$ = 200 000) as solute was purchased from Wako Pure Chemical Industries, Ltd. Tetrahydrofuran (THF, purity GC: min. 99.5 %) as solvent was purchased from Kanto Chemical Co., Ltd. Glass substrate (76 × 26 mm$^2$, thickness 1.0 mm) was purchased from Matsunami Glass Ind., Ltd., and PS substrate (40 mm diameter × 13 mm height) was purchased from Asahi Glass Co., Ltd (Science Products Dept., Iwaki). The bacterial fixative was glutaraldehyde (10%), purchased from Wako. Bacteria were cultured in trypticase soy broth (44011), purchased from bioMerieux SA.

**Film Formation.** The thin films were fabricated by breath figures, a method that exploits polymer self-assembly behavior to fabricate porous polymer thin films characterized by arrays of uniform pore size. The method is controlled by dropwise condensation in a high-humidity environment at ordinary temperatures and pressures.[26−28]

To obtain the solution, THF was mixed with PS at three different concentrations: 1, 3, and 5 wt %. The polymer thin films were fabricated by 1 mm$^3$/mm$^2$ cast-coating on the glass substrate at room temperature or cooled to 0 °C by cooling equipment (CPS-30, AS ONE Corporation) without the cover for samples A−D in Table 1 or with the cover for samples E−K in Table 1, and the coated substrates were set in a 23 °C thermo-hygrostat (PR-1KP, ESPEC Corp.) for 1 h (Figure 1). The humidity conditions of the equipment were set to 30, 50, 70, and 90%.

**Structural Analysis.** The surface structures were observed by a color 3D laser scanning microscope (VK-9710, Keyence) and a scanning electron microscope (SEM, S4700, Hitachi). The pore diameters were analyzed by the image analysis software Image-J (NIHimage).

**Figure 1.** Image of the film-forming equipment with the cover in the thermo-hygrostat.

**Bacterial Cultivation Test.** The films were assessed for bacterial cultivation of *P. aeruginosa* (Figure 2), a suspected leading cause of hospital infection. First, the films (10 × 15 mm$^2$) were immersed in 15 mL of culture media containing *P. aeruginosa* in a petri dish (38 mm diameter) and incubated for 1 week at 30−37 °C. Organisms were cultured in trypticase soy broth (44011) according to the manufacturer's instructions. The culture medium was then discarded, and weakly attached bacteria were removed by thrice rinsing with pure water. The bacteria adhered to the films were immobilized by glutaraldehyde for 1 day, washed, and observed under SEM. The area of film occupied by bacteria was estimated by Image-J processing of the SEM images.

## RESULTS AND DISCUSSION

**Microstructures of the Films Fabricated by Breath Figures.** Figure 3 illustrates how the porous structure is altered with PS concentration. As reported by Billon et al.,[53] the pore diameter reduces as the solution concentration increases.[54−56] This result is attributable to two phenomena. First, because the viscosity of the solution increases at high PS concentration, water droplets condensing on the surface are largely prevented from sinking into the solution. Second, because the thermal conductivity of PS is lower than that of THF, the water droplets condensing on the surface become smaller with increasing PS concentration.

The pore size of the films fabricated by breath figures also depends on relative humidity, as demonstrated by Brown et al.[57,58] According to Figure 4, the pore size increases as relative humidity increases. In addition, the depth to which water droplets sink into the solution depends on only the PS concentration and is independent of film structure. At higher humidity, larger water droplets condense on the cooled surface above the saturated water-vapor density. Larger water droplets readily sink into the film, generating a large-pore structure.

**Bacterial Proliferative Properties.** On the basis of the above results, we constructed films of various pore diameters by varying the concentration and humidity conditions (Table 1). Thereafter, samples for evaluating bacterial colonization were prepared under each experimental condition. Once the proliferative test was complete, the area covered by the bacteria and the average pore diameter were analyzed from SEM images (Figure 5). The white regions in the SEM images (the regions occupied by *P. aeruginosa*) appear red after applying the edge effect of SEM in Image-J processing. The antimicrobial properties of each film were assessed from the extent of bacterial occupation (Figure 6).

According to Figure 5A,B, *P. aeruginosa* biofilms occupy a large area (more than half of the substrate surface). Biofilms are microbial aggregates in which cells adhere to each other on a surface[59] and secrete extracellular polymeric substances (EPS). EPS encourages cellular aggregation and protects the internal cells from environmental changes and chemical substances. Biofilms can form on living or nonliving surfaces and are common sources of infection in natural, industrial, and hospital situations.[60,61] Under experimental conditions C−I, *P. aeruginosa* were fewer in abundance than under other conditions. In particular, under conditions E−H, few *P. aeruginosa* were found on the substrate surface (Figure 5). The organism proliferated more easily on large-pore films, but was prevented from forming biofilms.

Figure 7 indicates the relationship between the area covered by bacteria and the average pore diameter, determined by Image-J analysis of SEM images (Figsures 5 and 6). The area

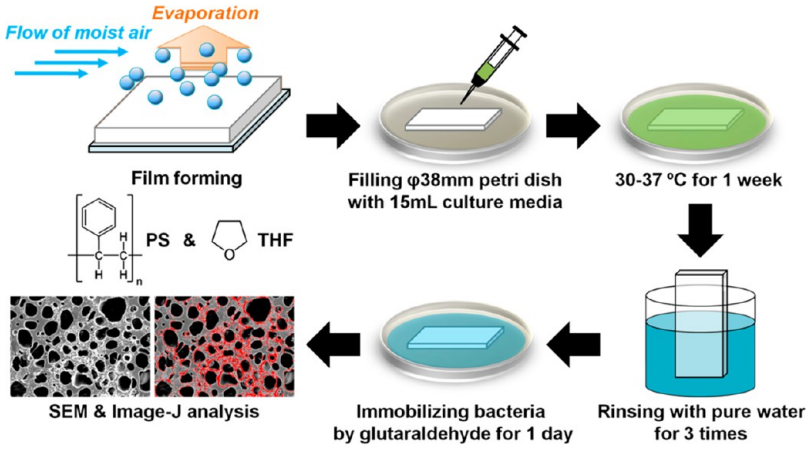


**Figure 2.** Schematic of experimental procedure from film formation to bacterial adhesion test.

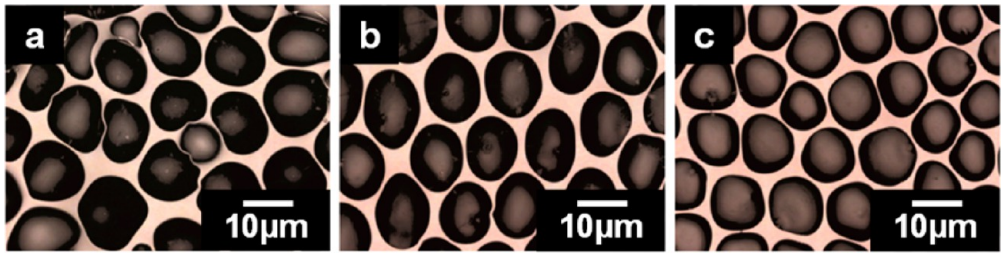


**Figure 3.** Changing porous structure in thin films fabricated at different PS concentrations. Shown are laser scanning microscope images at PS concentrations of (a) 1, (b) 3, and (c) 5 wt %. The PS substrates were cooled to 0 °C at 70 % relative humidity.

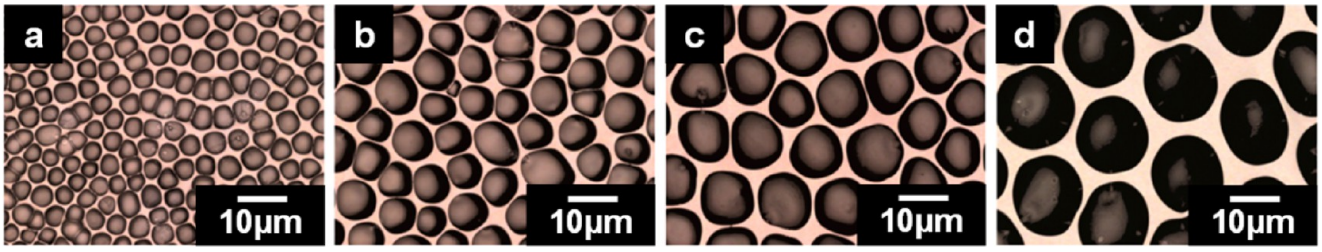


**Figure 4.** Changing porous structure in thin films fabricated at different humidity. Shown are laser scanning microscope images of the fabricated PS substrates at relative humidities of (a) 30, (b) 50, (c) 70, and (d) 90 %. Substrate temperature was maintained at 0 °C.

**Table 1. Experimental Conditions for Fabricating Each Sample Examined in the Antibacterial Activity Assay**

| sample name | concentration of PS (wt %) | relative humidity (%) | cover | temperature of substrate (°C) |
|---|---|---|---|---|
| A | 5 | 70 | none | 23 |
| B | 5 | 90 | none | 23 |
| C | 5 | 50 | none | 0 |
| D | 5 | 70 | none | 0 |
| E | 5 | 30 | with cover | 0 |
| F | 5 | 50 | with cover | 0 |
| G | 5 | 70 | with cover | 0 |
| H | 3 | 70 | with cover | 0 |
| I | 5 | 90 | with cover | 0 |
| J | 1 | 30 | with cover | 0 |
| K | 1 | 50 | with cover | 0 |

covered by biofilms was estimated from the area occupied by *P. aeruginosa* in images similar to panels A and B in Figure 5.

On films of pore diameter <3.5 μm, *P. aeruginosa* aggregated into biofilms that occupied more than half of the surface. No biofilms developed on films whose pore diameters ranged from 3.5 to 5 μm, although many bacteria adhered between the pores. When the pore size ranged from 5 to 11 μm, bacterial coverage was considerably reduced, reaching a minimum of 0.59% under experimental condition H. At larger pore diameters (>11 μm), bacterial coverage again increased, reaching 31.5% at the largest diameter. As observed for the smaller pore sizes, no biofilms appeared on the surfaces.

We now discuss the likely factors responsible for the above-mentioned antimicrobial trends (Figure 8). Initial adhesion by *P. aeruginosa* may depend on the extent to which bacterial culture media infiltrate the pores, which in turn depends on pore diameter. Wu et al.[62] reported that changing the pore diameter of porous structures alters the contact angle between the film and the culture medium. If the culture media has a low intrinsic contact angle on the films, then it will immediately spread and fill all of the pores. Following the initial spreading,

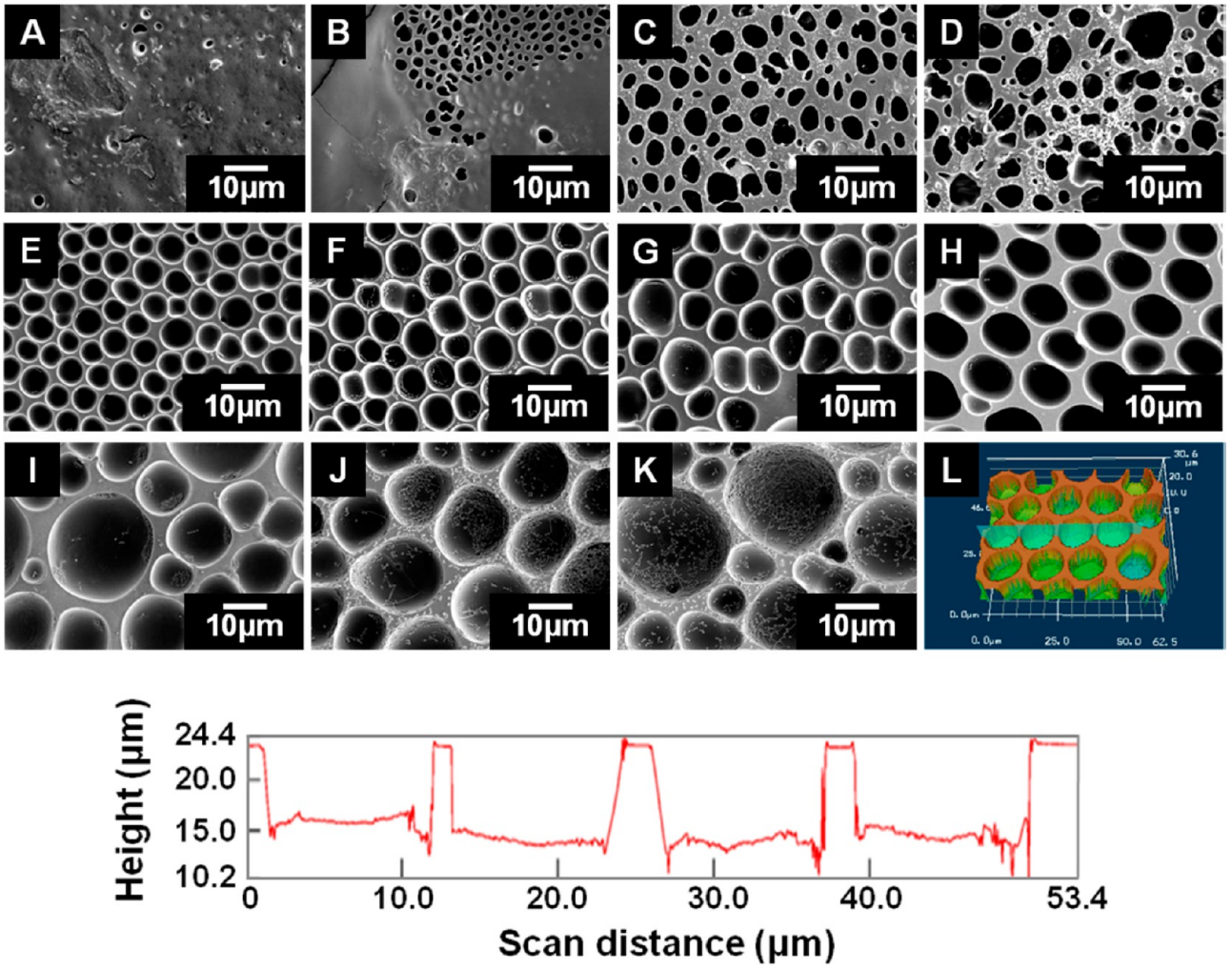


**Figure 5.** (A–K) SEM surface images collected after bacterial cultivation test. The experimental conditions under which each film is fabricated are listed in Table 1. The white parts are *P. aeruginosa*. (L) Color 3D laser scanning microscope image of panel H before the bacterial cultivation test. The green line indicates the height scan of the chart below.

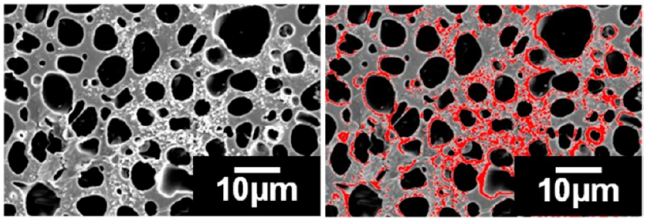


**Figure 6.** Characterization by Image-J. Bacterial adhesion appears as white patches in the left SEM image and as red patches after Image-J analysis (right).

Laplace pressures cause the concave liquid surfaces to grow by condensation and the convex surfaces to slowly evaporate. The final state is a surface covered by culture media with zero apparent contact angle and zero Laplace pressure. Conversely, if the intrinsic contact angle of the culture medium is high, all of the liquid surfaces are convex and evaporate under the Laplace pressure until their real contact area is zero. Laplace pressures also affect the liquid menisci, which depend on pore size. When bacterial culture is delivered dropwise into films with a porous structure, these two phenomena determine the contact area between *P. aeruginosa* and the films and may explain the minimal bacterial contact with the surface at intermediate pore sizes (5–11 μm).

Second, the pore diameter influences the potential field on microscale pores. As calculated by Everett et al.,[63] the van der Waals potentials of pore walls overlap when their size approximates the distance between walls, as occurs on microscale pores. In the current experiment, the films were immersed in bacterial culture media for 1 week, allowing the pores to become gradually infiltrated by the culture.[64] Accordingly, the force acting on *P. aeruginosa* as it penetrates the pores is influenced by the interaction potentials of the pore walls, which are pore-size-dependent. If the pore size is small (< 3.5 μm), *P. aeruginosa* readily forms biofilms atop the surface because individual cells collect and stabilize around pore gates. As the pore size increases from 3.5 to 11 μm, *P. aeruginosa* infiltrate the pores but is prevented from settling by the pore surface potentials. At large pore diameters (>11 μm), the influence of the potential is sufficiently weakened that *P. aeruginosa* can enter the pores.

Third, the physical barriers formed by breath figures critically control the movement of *P. aeruginosa* and retain trails of the extracellular polysaccharide Ps1 within the holes.[65] A recent study showed that *P. aeruginosa* secretes Psl during migration. The resulting Psl trails influence the motions of succeeding *P.*

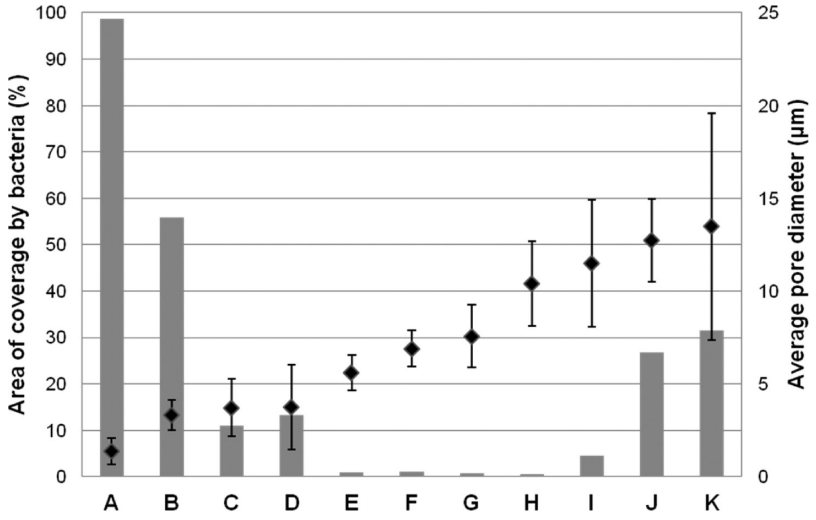


**Figure 7.** Relationship between the area covered by bacteria (gray bars) and the average pore diameter of films (black points), measured by Image-J analysis of SEM images A–K in Figure 4

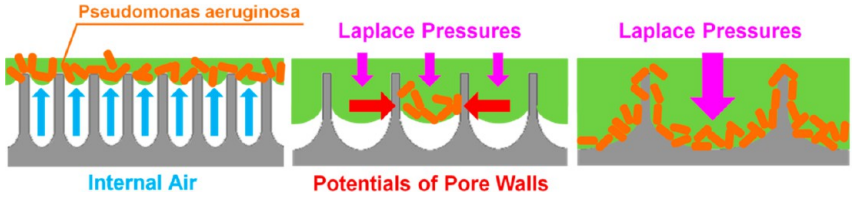


**Figure 8.** Antimicrobial model of porous films in this study: left, pore size less than ~3.5 μm; center, pore size ranging from 3.5 to 11 μm; and right, pore size exceeding 11 μm.

*aeruginosa* cells on the surface.[66] Structures with separated holes can disturb Psl trails and thereby weaken the ability of *P. aeruginosa* to colonize by attaching and self-organizing on the surfaces.

## CONCLUSIONS

This study investigated whether polymer thin films with porous structures fabricated by breath figures can be effective at biofilm formation inhibition and inhibition of bacterial adhesion surfaces. According to bacterial proliferation tests, at intermediate diameters of the arrayed pores (5–11 μm), the area covered by bacteria was minimized at 0.59 %, demonstrating that thin porous films effectively prohibit bacterial adhesion and growth at these pore diameters. To our knowledge, this study is the first report of a porous film, fabricated by breath figures at ordinary temperatures and pressures, that prohibits *P. aeruginosa* biofilm formation by controlling pore diameter. Environmentally friendly antimicrobial films are expected to be extensively researched in the future.

## ASSOCIATED CONTENT

### Supporting Information

Laser scanning microscope images color 3D laser scanning microscope images of the films at each PS concentration and each relative humidity; height scan of the films; relationship between PS concentration, humidity, and average pore diameter measured by Image-J analysis of laser scanning microscope images; cross-sectional image of (D); SEM surface images of various substrates after bacterial cultivation test. This material is available free of charge via the Internet at http://pubs.acs.org.

## AUTHOR INFORMATION

### Corresponding Author

*E-mail: shiratori@appi.keio.ac.jp.

### Notes

The authors declare no competing financial interest.

## ACKNOWLEDGMENTS

We thank the Terumo Corporation for their assistance in the bacterial cultivation test.

## REFERENCES

(1) Cotter, P. D.; Hill, C.; Ross, R. P. *Nat. Rev. Microbiol.* **2005**, *3*, 777–788.
(2) Morris, C. E.; Monier, J.-M. *Annu. Rev. Phytopathol.* **2003**, *41*, 429–453.
(3) Szewzyk, U.; Szewzyk, R.; Manz, W.; Schleifer, K.-H. *Annu. Rev. Microbiol.* **2000**, *54*, 81–127.
(4) Cleveland, J.; Montville, T. J.; Nes, I. F.; Chikindas, M. L. *Int. J. Food Microbiol.* **2001**, *71*, 1–20.
(5) Zhang, Y.; Mo, J.; Li, Y.; Sundell, J.; Wargocki, P.; Zhang, J.; Little, J. C.; Corsi, R.; Deng, Q. H.; Leung, M. H. K.; Fang, L.; Chen, W. H.; Li, J. G.; Sun, Y. X. *Atmos. Environ.* **2011**, *45*, 4329–4343.
(6) Gupta, K.; Hooyon, T. M.; Stamm, W. E. *Ann. Intern. Med.* **2001**, *135*, 41–50.
(7) Blajchman, M. A.; Goldman, M.; Baeza, F. *Transfus. Med. Rev.* **2004**, *18*, 11–24.
(8) Skovgaard, N. *Int. J. Food Microbiol.* **2007**, *120*, 217–224.
(9) Dharan, S.; Pittet, D. *J. Hosp. Infect.* **2002**, *51*, 79–84.
(10) Costerton, J. W.; Stewart, P. S.; Greenberg, E. P. *Science* **1999**, *284*, 1318–1322.
(11) Stewart, P. S.; Costerton, J. W. *Lancet* **2001**, *358*, 135–138.
(12) Andreeva, D. V.; Shchukin, D. G. *Mater. Today* **2008**, *11*, 24–30.

(13) Wang, G.; Zreiqat, H. *Materials* **2010**, *3*, 3994−4050.
(14) Lichter, J. A.; Van Vliet, K. J.; Rubner, M. F. *Macromolecules* **2009**, *42*, 8573−8586.
(15) Silver, L. L. *Curr. Opin. Microbiol.* **2003**, *6*, 431−438.
(16) Rizzello, L.; Sorce, B.; Sabella, S.; Vecchio, G.; Galeone, A.; Brunetti, V.; Cingolani, R.; Pompa, P. P. *ACS Nano* **2011**, *5*, 1865−1876.
(17) Dastjerdi, R.; Montazer, M. *Colloids Surf., B* **2010**, *79*, 5−18.
(18) Levy, S. B.; Marshall, B. *Nat. Med.* **2004**, *10*, S122−9.
(19) Wright, G. D. *Nat. Rev. Microbiol.* **2007**, *5*, 175−186.
(20) Podsiadlo, P.; Paternel, S.; Rouillard, J.-M.; Zhang, Z.; Lee, J.; Lee, J.-W.; Gulari, L.; Kotov, N. A. *Langmuir* **2005**, *21*, 11915−11921.
(21) Kumar, A.; Schweizer, H. P. *Adv. Drug Delivery Rev.* **2005**, *57*, 1486−1513.
(22) Bjarnsholt, T.; Jensen, P. Ø.; Burmølle, M.; Hentzer, M.; Haagensen, J. A. J.; Hougen, H. P.; Calum, H.; Madsen, K. G.; Moser, C.; Molin, S.; Hoiby, N.; Givskov, M. *Microbiology* **2005**, *151*, 373−383.
(23) Coates, A.; Hu, Y.; Bax, R.; Page, C. *Nat. Rev. Drug Discovery* **2002**, *1*, 895−910.
(24) Janek, T.; Lukaszewicz, M.; Krasowska, A. *Colloids Surf., B* **2013**, *110*, 379−386.
(25) Wang, H. H.; Ye, K. P.; Zhang, Q. Q.; Dong, Y.; Xu, X. L.; Zhou, G. H. *Food Control* **2013**, *32*, 650−658.
(26) Bunz, U. H. F. *Adv. Mater.* **2006**, *18*, 973−989.
(27) Srinivasarao, M.; Collings, D.; Philips, A.; Patel, S. *Science* **2001**, *292*, 79−83.
(28) Hoa, M. L. K.; Lu, M.; Zhang, Y. *Adv. Colloid Interface Sci.* **2006**, *121*, 9−23.
(29) Guadarrama-Cetina, J.; Gonzalez-Vinas, W. *Phys. Rev. E* **2013**, *87*, 054401.
(30) Leininger, S.; Olenyuk, B.; Stang, P. J. *Chem. Rev.* **2000**, *100*, 853−907.
(31) Ding, B.; Fujimoto, K.; Shiratori, S. *Thin Solid Films* **2005**, *491*, 23−28.
(32) Fukao, N.; Kyung, K. H.; Fujimoto, K.; Shiratori, S. *Macromolecules* **2011**, *44*, 2964−2969.
(33) Roberts, G. G. *Adv. Phys.* **1985**, *34*, 475−512.
(34) Zasadzinski, J. A.; Viswanathan, R.; Madsen, L.; Garnaes, J.; Schwartz, D. K. *Science* **1994**, *263*, 1726−1733.
(35) Acharya, S.; Hill, J. P.; Ariga, K. *Adv. Mater.* **2009**, *21*, 2959−2981.
(36) Decher, G. *Science* **1997**, *277*, 1232−1237.
(37) Shiratori, S. S.; Rubner, M. F. *Macromolecules* **2000**, *33*, 4213−4219.
(38) Matsuda, M.; Shiratori, S. *Langmuir* **2011**, *27*, 4271−4277.
(39) Ruokolainen, J.; Makinen, R.; Torkkeli, M.; Makela, T.; Serimaa, R.; ten Brinke, G.; Ikkala, O. *Science* **1998**, *280*, 557−560.
(40) Hajduk, D. A.; Harper, P. E.; Gruner, S. M.; Honeker, C. C.; Kim, G.; Thomas, E. L.; Fetters, L. J. *Macromolecules* **1994**, *27*, 4063−4075.
(41) Ma, M. L.; Hill, R. M.; Lowery, J. L.; Fridrikh, S. V.; Rutledge, G. C. *Langmuir* **2005**, *21*, 5549−5554.
(42) Pai, R. A.; Humayun, R.; Schulberg, M. T.; Sengupta, A.; Sun, J. N.; Watkins, J. J. *Science* **2004**, *303*, 507−510.
(43) Ariga, K.; Vinu, A.; Ji, Q. M.; Ohmori, O.; Hill, J. P.; Acharya, S.; Koike, J.; Shiratori, S. *Angew. Chem., Int. Ed.* **2008**, *47*, 7254−7257.
(44) Ariga, K.; Vinu, A.; Yamauchi, Y.; Ji, Q. M.; Hill, J. P. *Bull. Chem. Soc. Jpn.* **2012**, *85*, 1−32.
(45) Hernandez-Guerrero, M.; Stenzel, M. H. *Polym. Chem.* **2012**, *3*, 563−577.
(46) Gentili, D.; Foschi, G.; Valle, F.; Cavallini, M.; Biscarini, F. *Chem. Soc. Rev.* **2012**, *41*, 4430−4443.
(47) Nishikawa, T.; Nonomura, M.; Arai, K.; Hayashi, J.; Sawadaishi, T.; Nishiura, Y.; Hara, M.; Shimomura, M. *Langmuir* **2003**, *19*, 6193−6201.
(48) Nishikawa, T.; Nishida, J.; Ookura, R.; Nishimura, S. I.; Wada, S.; Karino, T.; Shimomura, M. *Mater. Sci. Eng., C* **1999**, *8*, 495−500.
(49) Ma, H. M.; Cui, J. W.; Chen, J. F.; Hao, J. C. *Chem.—Eur. J.* **2011**, *17*, 655−660.
(50) Greiser, C.; Ebert, S.; Goedel, W. A. *Langmuir* **2008**, *24*, 617−620.
(51) Goldmann, D. A.; Weinstein, R. A.; Wenzel, R. P.; Tablan, O. C.; Duma, R. J.; Gaynes, R. P.; Schlosser, J.; Martone, W. J. *JAMA* **1996**, *275*, 234−240.
(52) Ferrari, E.; Fabbri, P.; Pilati, F. *Langmuir* **2011**, *27*, 1874−1881.
(53) Billon, L.; Manguian, M.; Pellerin, V.; Joubert, M.; Eterradossi, O.; Garay, H. *Macromolecules* **2009**, *42*, 345−356.
(54) Li, L.; Chen, C.; Li, J.; Zhang, A.; Liu, X.; Xu, B.; Gao, S.; Jin, G.; Ma, Z. *J. Mater. Chem.* **2009**, *19*, 2789−2796.
(55) Ke, B.; Wan, L..; Chen, P.; Zhang, L.; Xu, Z. *Langmuir* **2010**, *26*, 15982−15988.
(56) Park, M. S.; Kim, J. K. *Langmuir* **2004**, *20*, 5347−5352.
(57) Brown, P. S.; Talbot, E. L.; Wood, T. J.; Bain, C. D.; Badyal, J. P. S. *Langmuir* **2012**, *28*, 13712−13719.
(58) Peng, J.; Han, Y. C.; Yang, Y. M.; Li, B. Y. *Polymer* **2004**, *45*, 447−452.
(59) Hall-Stoodley, L.; Costerton, J. W.; Stoodley, P. *Nat. Rev. Microbiol.* **2004**, *2*, 95−108.
(60) Karatan, E.; Watnick, P. *Microbiol. Mol. Biol. Rev.* **2009**, *73*, 310−347.
(61) Hoffman, L. R.; D'Argenio, D. A.; MacCoss, M. J.; Zhang, Z.; Jones, R. A; Miller, S. I. *Nature* **2005**, *436*, 1171−1175.
(62) Wu, X.; Wang, S. *ACS Appl. Mater. Interfaces* **2012**, *4*, 4966−4975.
(63) Everett, D. H.; Powl, J. C. *J. Chem. Soc., Faraday Trans.* **1976**, *72*, 619−636.
(64) Kabuto, T.; Hashimoto, Y.; Karthaus, O. *Adv. Funct. Mater.* **2007**, *17*, 3569−3573.
(65) Colvin, K. M.; Irie, Y.; Tart, C. S.; Urbano, R.; Whitney, J. C.; Ryder, C.; Howell, P. L.; Wozniak, D. J.; Parsek, M. R. *Environ. Microbiol* **2012**, *14*, 1913−1928.
(66) Zhao, K.; Tseng, B. S.; Beckerman, B.; Jin, F.; Gibiansky, M. L.; Harrison, J. J.; Luijten, E.; Parsek, M. R.; Wong, G. C. L. *Nature* **2013**, *497*, 388−391.